

Parametric and Non-Parametric Identification for an Automotive Air Conditioning System

Mohamed Ahmed Al-Awad
School of Mechanical Engineering,
Faculty of Engineering,
Universiti Teknologi Malaysia,
Johor, Malaysia

Zidan Abdul Ghani
School of Mechanical Engineering,
Faculty of Engineering,
Universiti Teknologi Malaysia,
Johor, Malaysia

Intan Z. Mat Darus
School of Mechanical Engineering,
Faculty of Engineering,
Universiti Teknologi Malaysia,
Johor, Malaysia
intan@utm.my

ABSTRACT

This research aims to develop the dynamic model of an Automotive Air Conditioning system using conventional and intelligent techniques. The research focused to achieve the optimal model that can effectively capture the behavior of the system. Linear and Non-Linear Autoregressive with Exogenous input (ARX and NARX) and Linear Autoregressive Moving Average with Exogenous inputs (ARMAX) models were used to capture the dynamics behavior of the system using system identification technique utilizing experimentally acquired input-output data. The system identifications were conducted using parametric and conventional method namely Recursive Least Squares (RLS) and Recursive Extended Least Squares (RELS), and nonparametric method using Intelligent algorithm of Multilayer Perceptron Neural Network. The comparative investigations have proven the superiority of the ARMAX model over the ARX and NARX model in term of prediction performance, whitening the disturbance as well as computational load for training. The mean square error are 2.7341×10^{-4} , 1.9017×10^{-5} and 5.0257×10^{-6} , for ARX, NARX, and ARMAX model respectively.

CCS CONCEPTS

CCS→Computing methodologies→Modeling and simulation→Model development and analysis→Modeling methodologies

KEYWORDS

automotive air conditioning system, system identifications, ARMAX, recursive least square, artificial neural networks

ACM Reference format:

Permission to make digital or hard copies of all or part of this work for personal or classroom use is granted without fee provided that copies are not made or distributed for profit or commercial advantage and that copies bear this notice and the full citation on the first page. Copyrights for components of this work owned by others than ACM must be honored. Abstracting with credit is permitted. To copy otherwise, or republish, to post on servers or to redistribute to lists, requires prior specific permission and/or a fee. Request permissions from Permissions@acm.org.
AIAM 2019, October 17–19, 2019, Dublin, Ireland
© 2019 Association for Computing Machinery. 978-1-4503-7202-2/19/10...\$15.00
<https://doi.org/10.1145/3358331.3358384>

Mohamed Ahmed Al-Awad, Zidan Abdul Ghani and Intan Z. Mat Darus. 2019. Parametric and Non-Parametric Identification for an Automotive Air Conditioning System. In *AIAM' 19: 2019 International Conference on Artificial Intelligence and Advanced Manufacturing, October 17–19,*

2019, Dublin, Ireland. ACM, New York, NY, USA, 7 pages.
<https://doi.org/10.1145/3358331.3358384>

1 INTRODUCTION

Heating Ventilation and Air Conditioning (HVAC) system vehicle types were invented to present a thermal comfort zone for the passengers inside the vehicle, but the problem faced by the researchers is excessive energy consumption.

Based on an investigation led by Laboratory of National Renewable Energy [1], around 26 billion liters of fuel per year is being consumed by the Automobile Air Conditioning systems (AAC) in USA, which equalize 5.5% of the whole transportation fuel consumption in the USA. AAC systems are designed to be controlled based on identified model, by regulating the flow of speed using a valve or controlling the airflow by a fan.

Various modelling and simulation approaches are now available to simulate the dynamics of the HVAC system with alternating levels of complication and ability. Majority of these methods require meaningful assumptions and idealizations with facilitation to become simpler to be applied, but this simplicity restricts their ability to realistically model and control the dynamic behavior of the system. On the other hand, some techniques need highly specific skill and experience to be implemented, as these two qualities are commonly not one of the usual experiences of Air Conditioning control plans set.

The process to go from an acquired data into a mathematical representation is necessary for studying system behavior due to the insufficiency of enhancing and controlling it with lack of earlier knowledges, this procedure was called system identification (SI), thereafter, the goal is to create adequate models from measured input and output data [2]. The necessity of system modelling led to many research movements in SI area for this past three decades. SI have been introduced and developed, where dozens of techniques and methods become basic tools in signal processing and computational.

The term system identification coined by Lotfi Zadeh in 1962 is a procedure to obtain a mathematical description of a system [3]. SI can be classified based on the prior knowledge of the system into; firstly, White Box Identification at which the model is completely known and it is possible to construct it entirely from the physical insight and earlier knowledge. Secondly, Grey Box Structures, where some physical insight is available, but many parameters need to be determined from observed data [4].

Finally, Black Box Identification which is the most common one, the model structure parameters completely unknown, and no physical insight to be implemented, but the model selected is one of the models that have high flexibility, so the parameters are only calculated from the input and output data [5].

For the past two decades, increased attention among researchers have led to utilizing conventional and intelligent algorithms for the modelling of HVAC system, white, grey and black box based numerous methods were implemented, Zajic et al. [6] developed grey box models for the electronic and thermostatic expansion valve, Hariharan et al. [7], adopted ARX based grey box model to simulate the behavior of an evaporator and compressor. A cooling coil and power consumption of a chiller system were modeled by Jin et al. [8] and Berardino et al. [9] respectively.

Artificial intelligent techniques were studied as well, where, Li et al. [10] employed Artificial Neural Networks (ANN) technique to model an air conditioning system, direct expansion types, while an AAC system was modelled by Ng et al. [11] using NARX based ANN model. Franco et al. [12] applied a Neuro-Fuzzy model for modelling and identifying the behavior of a non-linear dynamic condensing, evaporating and propylene glycol temperatures of a pilot refrigeration system.

2 MODELLING AND SIMULATING THE AAC SYSTEM

A. RELS based ARMAX model identification:

The mathematical description for the generalized structure of statistical black-box models in a simple correlation between input $\mathbf{u}(t)$, output $\mathbf{y}(t)$ and noise disturbance $\mathbf{e}(t)$, is expressed as follows:

$$\mathbf{A}(q^{-1})\mathbf{y}(t) = \frac{\mathbf{B}(q^{-1})}{\mathbf{F}(q^{-1})}\mathbf{u}(t) + \frac{\mathbf{C}(q^{-1})}{\mathbf{D}(q^{-1})}\mathbf{e}(t) \quad (1)$$

ARMAX model contains A, B, and C polynomial in its general formula equation as follows:

$$\mathbf{y}(t) = \frac{\mathbf{B}(q^{-1})}{\mathbf{A}(q^{-1})}\mathbf{u}(t) + \frac{\mathbf{C}(q^{-1})}{\mathbf{A}(q^{-1})}\mathbf{e}(t) \quad (2)$$

where, $\mathbf{A}(q^{-1})$, $\mathbf{B}(q^{-1})$ and $\mathbf{C}(q^{-1})$ are the model polynomials which are given as:

$$\begin{aligned} \mathbf{A}(q^{-1}) &= 1 + a_1q^{-1} + a_2q^{-2} + \dots + a_{na}q^{-n_a} \\ \mathbf{B}(q^{-1}) &= b_0 + b_1q^{-1} + b_2q^{-2} + \dots + b_{nb}q^{-n_b} \\ \mathbf{C}(q^{-1}) &= 1 + c_1q^{-1} + c_2q^{-2} + \dots + c_{nc}q^{-n_c}. \end{aligned} \quad (3)$$

while, (q^{-1}) is the back shift operator, \mathbf{n}_a , \mathbf{n}_b and \mathbf{n}_c are the polynomials $\mathbf{A}(q^{-1})$, $\mathbf{B}(q^{-1})$ and $\mathbf{C}(q^{-1})$ order respectively.

thus, (2) can be written in the following forms:

$$\begin{aligned} \mathbf{A}(q^{-1})\mathbf{y}(t) &= \mathbf{B}(q^{-1})\mathbf{u}(t) + \mathbf{C}(q^{-1})\mathbf{e}(t) \quad (4) \\ (1 + a_1q^{-1} + \dots)[\mathbf{y}(t)] &= (b_0 + b_1q^{-1} + \dots)[\mathbf{u}(t)] + \\ &\quad (1 + c_1q^{-1} + \dots)[\mathbf{e}(t)] \quad (5) \end{aligned}$$

one step ahead predicted (OSA) output can be estimated based on the following relation:

$$\begin{aligned} \hat{\mathbf{Y}}(t) &= [-\mathbf{y}(t-1), \dots, -\mathbf{y}(t-n_a); \mathbf{u}(t-1), \dots, \mathbf{u}(t- \\ &\quad n_b); \mathbf{e}(t-1), \dots, \mathbf{e}(t-n_c)] \begin{bmatrix} a_1 \\ \vdots \\ a_{na} \\ b_1 \\ \vdots \\ b_{nb} \\ c_1 \\ \vdots \\ c_{nc} \end{bmatrix} \quad (6) \\ \hat{\mathbf{Y}}(t+1) &= \boldsymbol{\varphi}(t) \hat{\boldsymbol{\theta}}(t) \quad (7) \end{aligned}$$

where, $\hat{\mathbf{Y}}(t+1)$, is the predicted output matrix, $\boldsymbol{\varphi}(t)$, is the coefficient matrix of the parameters to be identified, it also called (regression matrix), $\hat{\boldsymbol{\theta}}$, represents the estimated parameter matrix, \mathbf{d} is the delay value.

For each sample of the measured data t , the estimated parameter matrix $\hat{\boldsymbol{\theta}}$ was updated based on the online Recursive Extended Least Square (RELS) identification method [13][14].

RELS algorithm:

$$\begin{aligned} \mathbf{e}(t) &= \mathbf{y}(t) - \boldsymbol{\varphi}(t) \hat{\boldsymbol{\theta}}(t-1) \\ \mathbf{A}(t) &= \mathbf{P}(t-1) \boldsymbol{\varphi}(t) \\ \mathbf{D}(t) &= \lambda + \boldsymbol{\varphi}(t)^T \mathbf{A}(t) \\ \mathbf{L}(t) &= \frac{\mathbf{A}(t) \boldsymbol{\varphi}(t)^T}{\mathbf{D}(t)} \\ \hat{\boldsymbol{\theta}}(t) &= \hat{\boldsymbol{\theta}}(t-1) + \mathbf{L}(t)\mathbf{e}(t) \\ \mathbf{P}(t) &= \frac{1}{\lambda} [\mathbf{P}(t-1) - \mathbf{L}(t)\mathbf{P}] + \mu \mathbf{I}. \end{aligned} \quad (8)$$

in which, λ , is the forgetting factor which should be within range ($0 < \lambda < 1$), μ is the covariance resetting factor, \mathbf{I} is the identity matrix, and $\mathbf{P}(t)$, is a symmetric matrix, where, $\lambda \boldsymbol{\epsilon}(\mathbf{0}; \mathbf{1}]$, $\mathbf{P}(\mathbf{0}) = \mathbf{P}_0$, $\hat{\boldsymbol{\theta}}(\mathbf{0}) = \boldsymbol{\theta}_0$.

B. RLS based ARX model identification:

ARX model structure was also selected to simulate the dynamics behavior of the AAC system. The ARX model formula can be written as:

$$\mathbf{y}(t) = \frac{\mathbf{B}(q^{-1})}{\mathbf{A}(q^{-1})}\mathbf{u}(t) + \frac{1}{\mathbf{A}(q^{-1})}\mathbf{e}(t) \quad (9)$$

since the noise polynomial term C was ignored, then the disturbance term $\mathbf{e}(t)$ will not be excited, thus, the model assumed to describe the plant based only on the actual measured i/o data [15].

$$\mathbf{y}(t) = \frac{\mathbf{B}(q^{-1})}{\mathbf{A}(q^{-1})}\mathbf{u}(t) \quad (11)$$

$$\mathbf{A}(q^{-1})\mathbf{y}(t) = \mathbf{B}(q^{-1})\mathbf{u}(t) \quad (12)$$

using the same principle from polynomials equations set (3):

$$(1 + a_1q^{-1} + \dots + a_{na}q^{-n_a})[\mathbf{y}(t)] = (b_0 + b_1q^{-1} + \dots + b_{nb}q^{-n_b})[\mathbf{u}(t)] \quad (13)$$

thus, one step ahead (OSA) predicted output of ARX model can be obtained as following:

$$\hat{Y}(t) = [-y(t-1), \dots, -y(t-n_a); u(t-1), \dots, u(t-n_a)] \begin{bmatrix} a_1 \\ \vdots \\ a_{na} \\ b_1 \\ \vdots \\ b_{nb} \end{bmatrix} \quad (15)$$

In order to estimate the parameter vector $\hat{\theta}$, RLS identifier was adopted to update the parameter matrix at every single iteration, the algorithm steps is described as following [15], [16]

RLS algorithm:

$$\begin{aligned} A(t) &= P(t)\varphi(t) \\ L(t) &= \lambda + \varphi(t)^T A(t) \\ K(t) &= \frac{A(t)}{L(t)} \\ P(t+1) &= \lambda^{-1}P(t) + \lambda^{-1}k(t)\varphi(t)^T P(t) \\ \hat{\theta}(t+1) &= \hat{\theta}(t) + K(t)[y(t) - \varphi(t)^T \hat{\theta}(t)]. \end{aligned} \quad (16)$$

where:

$$\lambda \in (0:1], P(0) = P_0, \hat{\theta}(0) = \theta_0$$

C. Artificial Neural Networks (ANN) based NARX model:

The principal processing element of the artificial neural network is a neuron, while weighted connecting serves as in the synapses. The structure of the ANN model is made up of three layers, every layer contains a specific number of neurons, the input layer contains N number of neurons that refer to the number of inputs signal and same principle for the output and the hidden layers as shown in Figure 1.

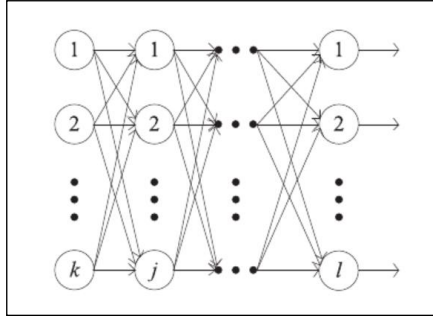


Figure 1: The general architecture of MLP Neural Networks [17].

where K, L, represents the number of neurons in the input and output layer respectively, which refers to the number of input and output variables, while j refers to the number of neurons in the first hidden layer until Nth hidden layers.

Every neuron received an input signal through weighted joints (inputs) and these inputs are summed in a particular manner. The formulation for the sum of the weighted inputs in given as:

$$n = \sum_{i=1}^r W_i P_i + b \quad (17)$$

where, P_i is the input matrix, W_i represent the weight connect indirectly the input with output, and b is the neuron bias. The

summation of the biases with the weighted inputs is introduced through a function called the activation function, symbolize as f , in order to estimate the output based on the following formula (14)[18]:

$$y(n) = f \left[\sum_{i=1}^r (W_i P_i + b) \right] \quad (18)$$

Multilayer perceptron (MLP) Network based NARX model was implemented with input, $y(t-1)$ which is the previous output for time series at the time $(t-1)$, and additional input $x(t-1)$ with exogenous data at time $(t-1)$, in order to obtain one estimated output $y(t)$, parallel to the one step ahead predicted output value

Figure 2, shows MLP based NARX architecture with the exogenous principle, where the estimated $y(t)$ depends on the outer value as in the following formula.

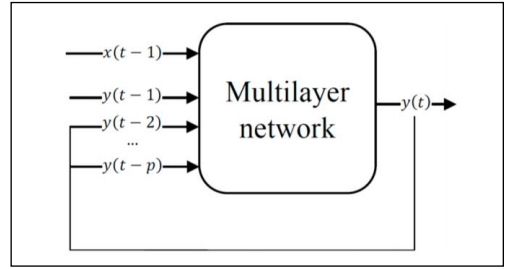


Figure 2: MLP based NARX model scheme

The following equation represent the NARX structure [19]:

$$y(t) = f^1 [x(t-1)x(t-2), \dots, x(t-q); y(t-1)y(t-2), \dots, y(t-p)] \quad (19)$$

where, q and p are the maximum time lag for the input and output respectively which called delay number, $y(t)$ and $u(t)$ are the output and input sequence of the system, f^1 is a nonlinear function used to introduce the non-linearity of the system into the neural networks, which considered to be Tan-Sigmoid activation function (tansig).

Based on the description for the NARX model, the lagged value of the estimated outputs and exogenous inputs are provided through the training step. Levenberg–Marquardt methods was utilized to train the networks in which weights are adjusted with the following rule:

$$W_{m+1} = W(m) + (J(m)^T J(m))^{-1} J(m)^T e(m) \quad (20)$$

3 RESULTS AND DISCUSSION

A. Parametric Identification results:

Both, ARMAX and ARX model characters; model order and forgetting factor influence on the model performance were studied in this section in order to obtain the optimal models structure. Therefore, 11363 samples of experimental data that collected by Mat Darus [19] with frequency rate of 1 were used. The empirical data were divided into two data set, first 9000 samples were taken for training purpose and the remaining input-output data for testing.

For RLS based ARX model, the model order was fixed at 2, and the forgetting factor (λ) was varied among the range 0.1 to 0.9,

where λ is a constant value, its main function is to provide a greater weight for the new estimated output value of the system. It also encourages the solution to search and heads toward quickly to the global minimum. While for RELS based ARMAX model, the forgetting factor is in the range of 0.9 to 0.98 rather than the range of 0.1 to 0.9, in order to avoid the covariance matrix blow up problem in the algorithm, while the order of the model was fixed at 2nd order, the results was tabled in Table 1,

Table 1: Performance of parametric identification models

ARX model		ARMAX model		M.O	ARX	ARMAX
λ	MSE ($\times 10^{-6}$)	λ	MSE ($\times 10^{-4}$)		MSE ($\times 10^{-4}$)	
0.1	3.84038	0.98	0.054581	2	2.73404	0.050257
0.2	2.95146	0.97	0.059816	3	4.32648	0.073165
0.3	2.95448	0.96	0.068187	4	5.80097	0.116501
0.4	3.08952	0.95	0.075833	5	7.25733	0.178413
0.5	3.30006	0.94	0.080634	6	8.73772	0.225308
0.6	3.47030	0.93	0.081027	7	10.2703	0.267102
0.7	3.43540	0.92	0.075322	8	11.8856	0.316466
0.8	3.14383	0.91	0.063432	9	13.5658	0.367607
0.9	2.73404	0.90	0.050257	10	15.2581	0.415979

The analysis is continued by examining the effect of the model order which it reflects on the model parameters of the polynomials; $A(q^{-1})$, $B(q^{-1})$ and $C(q^{-1})$, where it was varied up to 10th order.

The results have shown that the lowest mean square error by testing the forgetting factor was obtained when the forgetting factor is 0.9 for both models. However, it should be noticed that the ARX model parameters disposed to have slight fluctuation, and as we increase λ it is starting to converge as shown in Figure 3. Due to the fluctuation it leads to a high fluctuation in the predicted error for the ARX model as in Figure 5, while ARMAX model parameters converged quickly as in Figure 4. The estimated data obtained by ARX and ARMAX models are both in high-grade agreement with the actual data of the cabin temperature of AAC system as in Figure 7, which proved its capability to estimate the temperature through the training and testing phase.

Based on unit circle stability analysis, it was found that all the poles are located within the unit circle as in Figure 8 for both parametric models which indicates stable models.

Figures 9(a) and 9(b) illustrate the correlation tests results for ARX and ARMAX models, respectively. The first four graphs illustrate the linear part of the correlation tests, it can be observed that the relationship between the predicted error with the input and with itself proportionally to the shifted copies of the output are relatively within the confidence range. As expected, the ARX model predicted residual is relatively confined to the bounds of the confidence intervals for all of the equation sets while the ARMAX model perform perfectly for the nonlinear part of the statistical tests; $\hat{\sigma}_{u^2e}(\tau)$, $\hat{\sigma}_{u^2e^2}(\tau)$ and $\hat{\sigma}_{e(eu)}(\tau)$, comparing to the ARX model for testing data set record as shown in Figure 9.

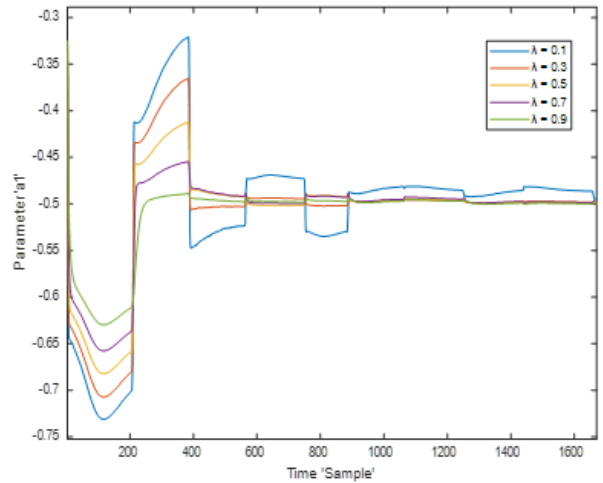


Figure 3: Parameter fluctuation under different values of λ for ARX model.

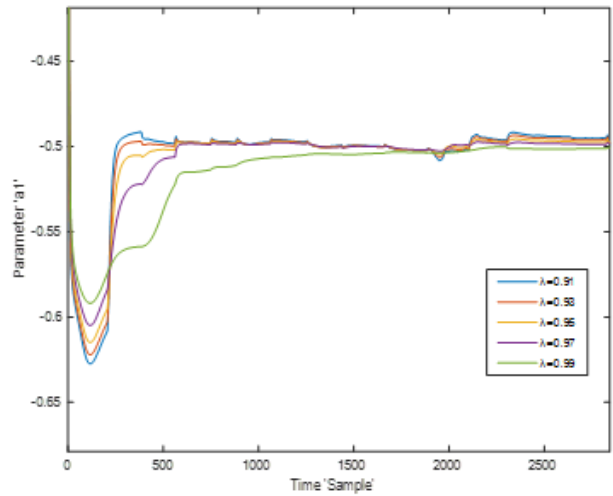


Figure 4: Parameter fluctuation under different values of λ for ARMAX model.

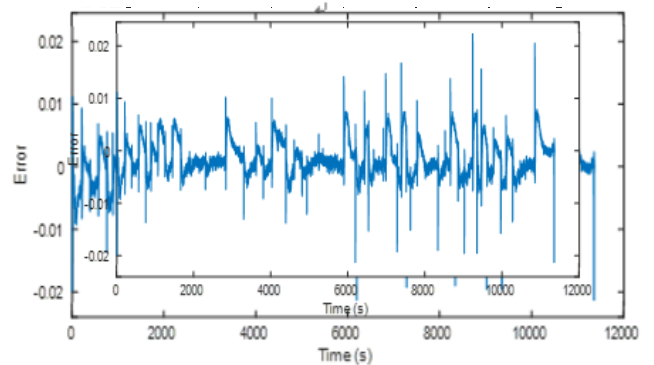


Figure 5: Predicted error by online RLS based ARX model.

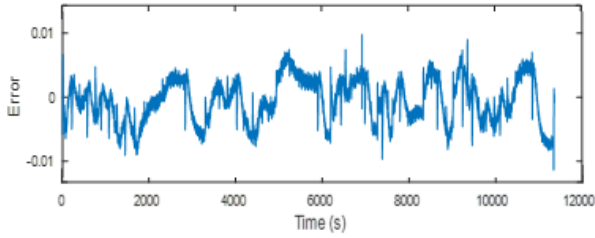


Figure 6: Predicted error by online RELS based ARMAX model.

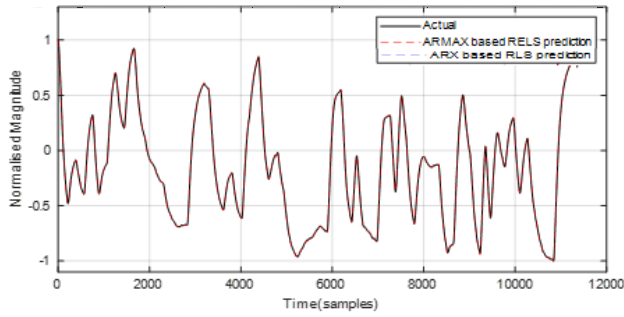


Figure 7: Actual versus predicted output via ARX and ARMAX model.

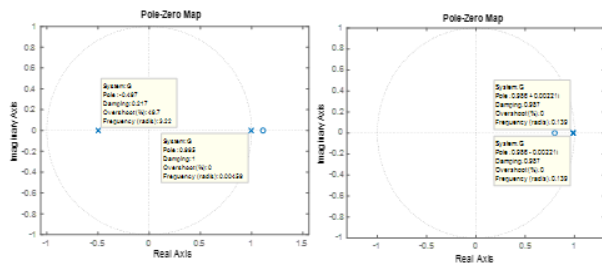


Figure 8: Unit circle stability analysis ARX and ARMAX respectively.

B. Non-Parametric Model Results:

The optimal NARX-Neuro structure was accomplished by altering three characters; the number of the hidden layer, number of delays, and neurons numbers per hidden layer. It is common to say, the neuro structure was determined through the trial-and-error procedure since there is no a methodical approach, where some investigations explicate that one or two hidden layers may result in good convergence.

The number of neurons was varied coincidentally with the delay number while fixing the hidden layer number at 1, 2 and 3 layers in term of Mean Square Error via One Step Ahead prediction (OSA) as illustrated in Figure 10.

However, from Figure 10, it can be observed that for the first four increments of the neurons, significant reduction of the MSE takes place up to a certain limitation, then suddenly the MSE starts to increase when the neurons go beyond 12 neurons per hidden layers. it can be stated obviously, increasing the neurons overmuch influence the generalization capability of the neuro structure and extends the computational load.

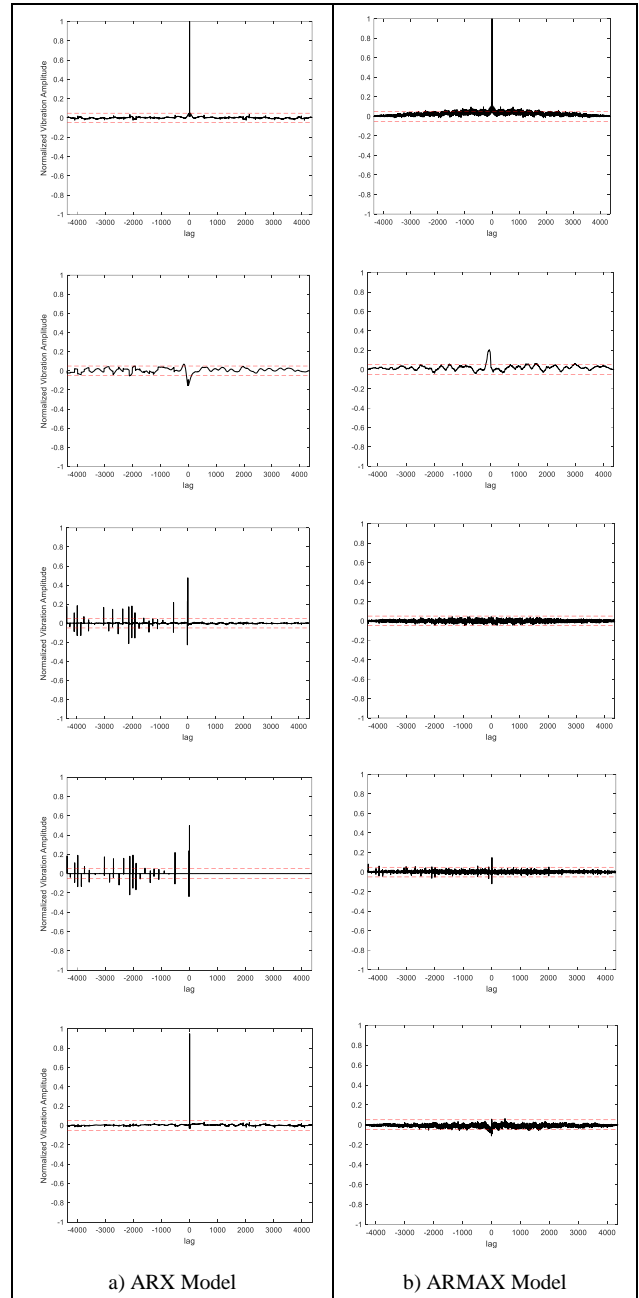


Figure 9: Correlation tests.

The best MSE was achieved when there are 12 neurons with one hidden layer while the delay is 2 for input and output; is (1.90172×10^{-5}) and the time consumed to train the network was 39.985 seconds.

The predicted output by the NARX via NN model is almost fitted to the actual data of the cabin temperature variable of the AAC system where the regression value R was found to be **0.99993** to the actual data as in Figure 11 and Figure 12, the model was found to be unbiased based on the statistical tests where the residual is relatively within the confidence bounds as shown in Figure 13.

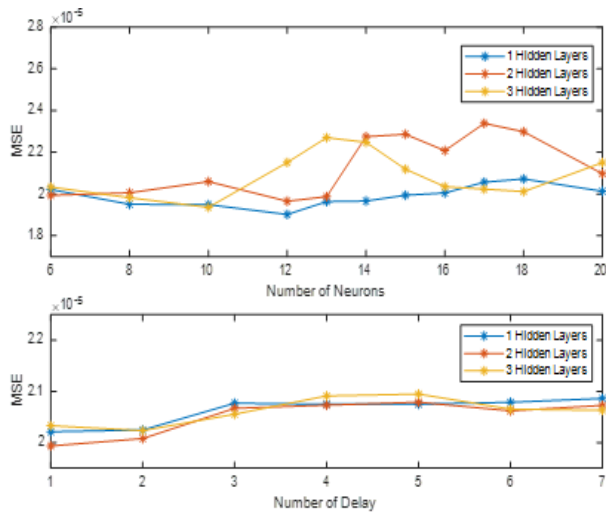


Figure 10: MLP networks performance under different structures.

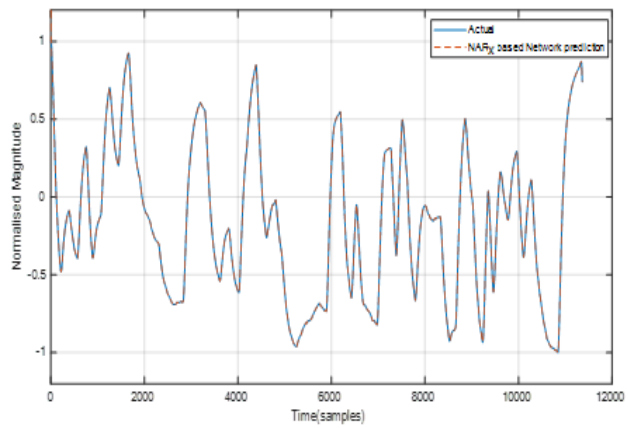


Figure 11: Actual versus predicted output via Multilayer perceptron networks.

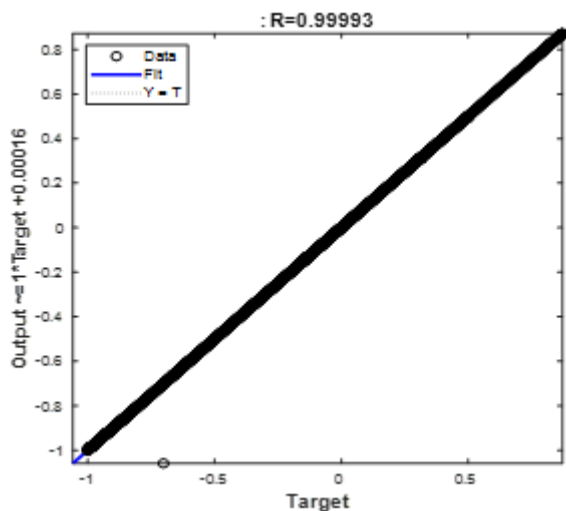


Figure 12: Regression Plot of Multilayer perceptron based NARX model.

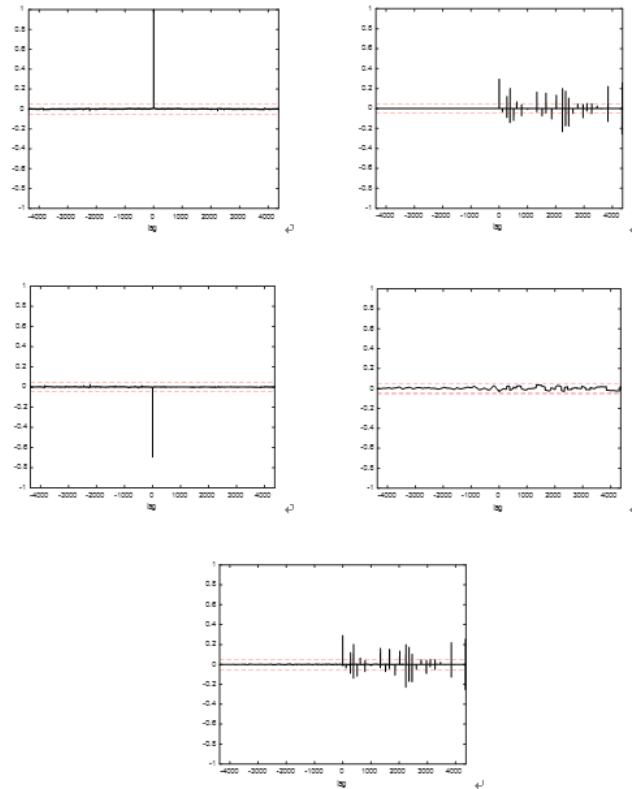


Figure 13: Correlation tests of Multilayer perceptron based NARX.

4 CONCLUSION

Performance comparison between the ARMAX model identified using RELS, ARX model based RLS, and NARX model via MLP in different model orders, forgetting factor, delay value, neurons and hidden layer numbers in term of mean square error (MSE) of residuals due to one step ahead prediction (OSA) were studied and the results were obtained.

The lowest MSE for all three models were achieved by 2nd order ARMAX model based RELS with forgetting factor of 0.9, 2nd order ARX model based RLS with forgetting factor of 0.9 and MLP network with one hidden layer consists of 12 neurons while the delay is two. The lowest mean square errors were 5.0257×10^{-6} , 2.7341×10^{-4} , and 1.9017×10^{-5} for ARMAX, ARX and NARX respectively. On the other hands, the simulation time consumed by MLP is highest compared to other identifiers, while the regression value is almost tending to one for all estimated models.

The AAC system requires a robust model that can deal with a wide kind of disturbance, from statistical tests we can state that, ARMAX model is further comprehensive, complementary and obviously a good option for such system compared to ARX and NARX model based on residual analysis, at which the ARMAX has high ability to turn the disturbance almost into a white noise, where the estimated residuals in ARMAX was applied to predict the exogenous disturbance variable, since the Recursive Extended Least Square method is well-known to whiten the residuals in availability of a well-modelled disturbance variable.

Therefore, in conclusion, for the AAC system studied in this research, the ARMAX model based RELS has higher tractability to model the disturbances affects compared to ARX model based RLS and NARX model via MLP networks with the lowest MSE prediction error of 5.0257×10^{-6} .

REFERENCES

- [1] J.P. Rugh, L. Chaney, J. Lustbader and J. Meyer, 2007. Reduction in vehicle temperatures and fuel use from cabin ventilation, solar-reflective paint, and a new solar-reflective glazing SAE Technical Paper (No. 2007-01-1194).
- [2] L. Ljung, System Identification—Theory for the User, 2nd ed., Prentice Hall, Upper Saddle River, NJ, 1999.
- [3] T. Söderström, P. Stoica, System Identification, 2001st Edition, Series in Systems and Control Engineering, Prentice Hall, New York, 1989.
- [4] H.J. Tulleken, 1993. Grey-box modelling and identification using physical knowledge and Bayesian techniques. *Automatica*, 29(2), 285-308.
- [5] A. Juditsky, H. Hjalmarsson, A. Benveniste, B. Delyon, L. Ljung, J. Sjöberg and Q. Zhang, 1995. Nonlinear black-box models in system identification: Mathematical foundations. *Automatica*, 31(12), 1725-1750.
- [6] I. Zajic, T. Larkowski, M. Sumislawska, K.J. Burnham and D. Hill, 2011. Modelling of an air handling unit: a Hammerstein-bilinear model identification approach. 21st International Conference on Systems Engineering (ICSEng), 59-63.
- [7] N. Hariharan and B.P. Rasmussen, 2010. Parameter estimation for dynamic HVAC models with limited sensor information, American Control Conference (ACC), 5886-5891.
- [8] G.Y. Jin, P.Y. Tan, X.D. Ding and T.M. Koh, 2011. Cooling coil unit dynamic control of in HVAC system, 6th IEEE Conference on Industrial Electronics and Applications (ICIEA), 942-947.
- [9] J. Berardino and C. Nwankpa, C., 2010. Dynamic load modeling of an HVAC chiller for demand response applications. 1st IEEE International Conference on Smart Grid Communications (SmartGridComm), 108-113.
- [10] N. Li, L. Xia, D. Shiming, X Xu, M-Y. Chan, 2012. Dynamic modeling and control of a direct expansion air conditioning system using artificial neural network, *Applied Energy*, 91(1), 290-300.
- [11] B.C. Ng, I.Z. Mat Darus, H. Jamaluddin H. M. Kamar, 2014, Dynamic modelling of an automotive variable speed air conditioning system using nonlinear autoregressive exogenous neural networks, *Applied Thermal Engineering*, 73(1), 1255-1269.
- [12] I.C. Franco, M. Dall'Agnol, T.V. Costa, A.M.F. Fileti and F.V. Silva, 2011. A neuro-fuzzy identification of non-linear transient systems: Application to a pilot refrigeration plant, *International Journal of Refrigeration*, 34(8), 2063-2075.
- [13] J.C. Atuonwu, Y. Cao, G.P. Rangaiah and M.O. Tadé, 2010. Identification and predictive control of a multistage evaporator. *Control Engineering Practice*, 18(12), 1418-1428.
- [14] G.C. Goodwin and K.S. Sin, 2014. Adaptive filtering prediction and control. Courier Corporation.
- [15] J.B. Michaud, R. Fontaine and R. Lecomte, 2003. ARMAX model and recursive least-squares identification for DOI measurement in PET. *IEEE Nuclear Science Symposium Conference Record*, 4, 2386-2390.
- [16] I.Z. Mat Darus and M.O. Tokhi, 2006. Parametric and non-parametric identification of a two dimensional flexible structure. *Journal of Low Frequency Noise, Vibration And Active Control*, 25(2), 119-143.
- [17] B. Lindoff and J. Holst, 1999. Convergence analysis of the RLS identification algorithm with exponential forgetting in stationary ARX-structures. *International Journal Of Adaptive Control And Signal Processing*, 13(1), 1-22.
- [18] L. Wan, J. Liu, J. Harkin, L. McDaid and Y. Luo, 2017. Layered tile architecture for efficient hardware spiking neural networks. *Microprocessors and Microsystems*, 53, 21-32.
- [19] Ng, B.C., Darus, I.Z.M., Jamaluddin, H. and Kamar, H.M., 2014. Application of adaptive neural predictive control for an automotive air conditioning system, *Applied Thermal Engineering*, 73(1), 1244-1254.